and the repetition rates are 10 Hz for the both lasers. Figure 7 shows measured quantities of ablation when the two lasers irradiate the sample simultaneously and independently. The result "independent" is the sum of the ablation weight for the two lasers that were separately measured. The ablation quantities linearly increase with number of laser pulses and we found that the ablation efficiency is around 20% higher in the simultaneous irradiation. Figure 8 shows cutting sections of alumina balls ablated with Ho:YAG and Er:YAG lasers. With the Er:YAG laser light, the ablation proceeds to depth direction and the stress of the ablation brings destruction of the surface. For the Ho:YAG laser, in contrast, ablation uniformly occurs in lateral direction. When these two lasers irradiate the tissue simultaneously, the ablation occurs in both of depth and lateral directions and, as a result, the high ablation capability is obtained.

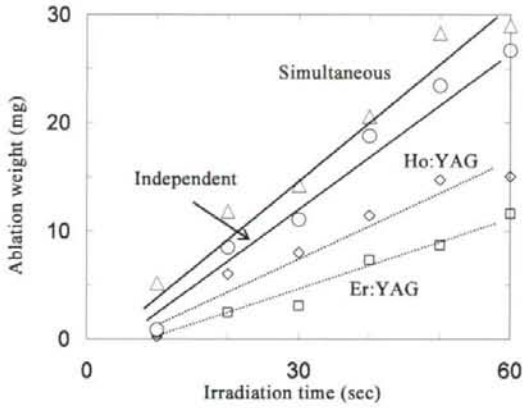

Fig. 7 Ablation weight after irradiated with two lasers simultaneously and independently

(a) Er:YAG (b) Ho:YAG (c) Er:YAG + Ho:YAG

Fig. 8 Cutting section of alumina balls ablated with Er:YAG and Ho:YAG lasers

3. Conclusion

Laser ablation experiments on hard tissues are performed by guiding combined beam of Ho:YAG and Er:YAG laser light with a hollow optical fiber. An alumina ball is used as a hard-tissue model and ablation phenomenon are observed by an ultra-high-speed camera. The result show that the two laser light give dissimilar ablation effects due to different absorption coefficient in water contained in the tissues. When the two lasers are combined and irradiate on the model, a high ablation rate is observed. In the experiments shown in this paper, the pulses of the two different lasers are not synchronized. Much higher effect of simultaneous irradiation is expected if they are synchronized and the pulse timing is finely tuned to maximize the effect. The experiment is carried on in our group and the result will be reported elsewhere.

References

1. A. Aoki, et al., "Comparison between Er:YAG laser and Conventional Technique for Root Caries Treatment in vitro," J. Dent. Res., **77**, 1404-1414 (1998)
2. M. K. Yiu, et al., "Clinical Experience With Holmium:YAG Laser Lithotripsy of Ureteral Calculi," Lasers Surg. Med., **19**, 103-106 (1996)
3. H. Lee, et al., "Urinary calculus fragmentation during Ho:YAG and Er:YAG lithotripsy," Lasers Surg. Med., **38**, 39-51 (2006)
4. K. F. Chan, et al., "Free Electron Laser Ablation of Calculi: An Experimental Study," IEEE J. Quantum Electron., **7**, 1022-1033 (2001)
5. T. Amagai, et al., "An Experimental Pathologic Study of Gingivectomy Using Dual-Wavelength Laser Equipment With OPO," Lasers Surg. Med., **39**, 51-58 (2007)
6. M. Miyagi, et al., "Design theory of dielectric-coated circular metallic waveguides for infrared transmission," J. Lightwave Technol., **LT-2**, 116-126 (1984)
7. K. Iwai, et al., "Erbium:YAG laser lithotripsy by use of a flexible hollow waveguide with an end-scaling cap," Appl. Opt., **42**, 2431-2435 (2003)

Thin Hollow Glass Waveguide for Near IR Radiation Delivery

Michal Němec[a*], Helena Jelínková[a], Jan Šulc[a]
Mitsunobu Miyagi[b], Katsumasa Iwai[b], Yi-Wei Shi[c], Yuji Matsuura[d]
[a]Faculty of Nuclear Sciences and Physical Engineering
Czech Technical University, Břehová 7, 115 19 Prague 1, Czech Republic
[b]Sendai National College of Technology, Aoba-ku, Sendai, 989-3128, Japan
[c]School of Information Science and Engineering, Fudan University, Shanghai, 200433, China
[d]Graduate School of Engineering, Tohoku University, Sendai 980-8579, Japan

ABSTRACT

The delivery of the radiation by thin fiber is required for some application, especially in medical internals treatment. Therefore a new 100 μm and 250 μm inner diameter hollow glass waveguides were developed and investigated for the possibility to transport high power near infrared laser radiation without damage of these delivery systems. As laser sources two Nd:YAG laser systems working in Q-switched regime at wavelength 1.06 μm and 1.34 μm were utilized. Delivered radiation characterization was performed. By Alexandrite laser (755 nm) pumped Q-switched Nd:YAG laser has been generating 1.06 μm wavelength radiation with 6 ns length of pulse and maximum output energy 0.7 mJ (116.7 kW). The laser was Q-switched using $LiF:F^{2-}$ saturable absorber. Second laser system was Nd:YAG/V:YAG microchip pumped by laser diode operating at 808 nm. The radiation at 1.3 μm wavelength has been generated with 250 Hz repetition rate. Pulse length was 6 ns and mean output power 25 mW. Corresponding pulse energy and peak power was 0.1 mJ and 16.7 kW, respectively. Both lasers were operating in fundamental TEM_{00} mode ($M^2 \sim 1$). For delivery a special cyclic olefin polymer-coated silver hollow glass waveguides with the inner/outer diameters 100/190 μm and 250/360 μm were used. The delivery system was consisted of lens, protector, and waveguide. As results the transmission more than 55 % and reasonable spatial profile of laser output radiation were found. From these measurements it can be recommended using of this system for near infrared powerful radiation delivery as well as for medical treatment.

Keywords: Hollow glass waveguide, IR lasers, spatial structure.

1. INTRODUCTION

Detailed knowledge of interaction beam spatial structure can be lead to precise laser applications in the medicine, industry, and also their use in research laboratories. Generally an articulated arm, optical fiber, and hollow waveguide are used as delivery systems of laser beam. Poor manipulability of the articulated arms reduces their utilization[1]. And for high power pulses, the third delivery type appears the best due to air core, high power damage threshold, low insertion losses, no end reflection, so we focused to hollow glass waveguides.

New waveguide types are investigated and better transfer properties of hollow waveguides are still developed[2-4]. The interaction beam spatial structure is another significant parameter and together with dimension of waveguides can define final application. So for ophthalmology, urology, dentistry or micro-surgery, the delivery of the radiation by thin waveguide is requested.

In the last year, we reported delivered systems with waveguide diameter of 700/850 μm[5]. The modification of the beam spatial structure during the propagation through the waveguide (cyclic olefin polymer coated silver hollow glass waveguide) was investigated for near and mid infrared radiation – 1.98 μm, 2.01 μm and 2.94 μm wavelength. The defined beam profile (approximately Gaussian mode) from the laser systems was changed into many peak structures having dominant intensity in the center.

* michal.nemec@fjfi.cvut.cz; phone +420 224 358 672; fax +420 222 512 735;

Optical Fibers and Sensors for Medical Diagnostics and Treatment Applications VIII,
edited by Israel Gannot, Proc. of SPIE Vol. 6852, 68520W, (2008) · 1605-7422/08/$18
doi: 10.1117/12.761837

The aim of the this work was to investigate the delivery high peak power near-infrared radiation (1.06 μm and 1.34 μm wavelength) by 100/190 μm and 250/360 μm thin hollow glass waveguides and the modification of the beam spatial profile, as well as the possibility of its utilization in medical application.

2. MATERIALS AND METHODS

2.1. Laser sources

2.1.1. Alexandrite laser radiation pumped Nd:YAG laser

The first Nd:YAG laser, operating at wavelength 1.06 μm, was coherently pumped by Alexandrite laser (755 nm emission wavelength, 30 mJ output energy, pulse duration 50 μs). As a laser active medium 60 mm long Nd:YAG rod was used (1 at.% Nd/Y, diameter 5 mm, AR/AR-coated faces). The pumping beam was focused into this crystal by a lens with 150 mm focal length. The crystal was placed into the 110 mm long linear resonator. The semihemispherical laser cavity was formed by a pumping spherical mirror and by flat output coupler. The pumping mirror (radius r = 500 mm) had high transmittance at the pumping (740–750 nm) wavelength and maximal reflectance at the oscillating wavelength about 1 μm. The output coupler reflectance was 60 % @ 1064 nm. Neodymium laser was Q-switched using LiF:F_2^- saturable absorber (T_0 ~ 70 %) which was placed inside the resonator between Nd:YAG rod and the output coupler. This configuration allows us to obtain stable well reproducible short powerful giant pulses.

Laser repetition rate of 5 Hz was done by repetition rate of Alexandrite laser power supply. The maximum output energy (peak power) and pulse length were 0.7 mJ (116.7 kW) and 6 ns, respectively. Laser was operating in a fundamental TEM_{00} mode (M^2 ~ 1). Generated radiation was unpolarized.

2.1.2. Diode pumped Nd:YAG/V:YAG laser

The second laser system was based on diode pumped Nd:YAG/V:YAG laser microchip, operating at wavelength 1338 nm[6]. This laser used specially developed sandwich crystal which combined in one piece the cooling undoped part (undoped YAG crystal 4 mm long), the active laser part (YAG crystal doped with Nd^{3+} ions, c = 1.1 % Nd/Y, 12 mm long), and the saturable absorber (YAG crystal doped with V^{3+} ions 0.7 mm long). The diameter of this crystal was 5 mm. The microchip resonator consisted of dielectric mirrors which were deposited directly on the monolith crystal surfaces. The pump mirror with the high transmission for pump radiation and the high reflection for generated radiation was placed on the undoped YAG part. The output coupler with reflectivity 90 % for the generated wavelength was placed on the V^{3+}-doped part. The total microchip laser resonator length was 16.7 mm. For this laser pumping a laser diode HLU20F400 (LIMO Laser Systems) was used. The diode was emitting radiation at wavelength 808 nm with the maximum output power 20 W at the end of the fiber (fiber core diameter: 400 μm; numerical aperture: 0.22). This radiation was focused into the active Nd:YAG crystal by two achromatic doublet lenses (focal length f = 75 mm). The laser diode was operating in pulsed regime (rep. rate 250 Hz, pulse width 300 μs, pulse energy 6 mJ) with duty-factor 7.5 % to reduce thermal effects inside the microchip laser.

Using this laser, stable and high reproducible Q-switched pulses were generated at wavelength 1338 nm. Pulse length was 6 ns (FWHM). The output mean power was 25 mW which corresponds to single pulse energy and peak power 0.1 mJ and 16.7 kW, respectively. The laser was operating in the fundamental TEM_{00} mode ($M^2 \cong 1$).

2.2. Delivery system – hollow glass waveguide

In this work, a polymer coated silver hollow glass waveguides were utilized as the delivery system. The waveguides consist of a fused silica glass tube coated inside with silver layer covered by a dielectric layer. This layer enhances the reflectance of transmitted light on the inner surface of the waveguide. As dielectric coating material, a cyclic olefin polymer (COP) was chosen. The thickness of dielectric film can be realized from 0.1 μm depending on the transmitted wavelength of radiation. The COP silver hollow glass waveguides were successfully produced with the length up to 2 m and with 1 mm, 700 μm, 540 μm, and 320 μm inner diameters. A polyimide protective layer was used on the fused silica tube outside surface. The mechanical strength of the waveguides was determined by the silica glass tubing.

New manufactured samples (investigated in this work) had the inner diameters 100 μm and 250 μm, and the outer diameters 190 μm and 360 μm, respectively. The length of trial samples was 10 cm. At disposal it was one 100 μm (1A6-11-2) and four 250 μm (C25-3-0, C25-3-1, C25-3-2, C25-3-4) waveguides. A very good flexibility done by thin silica glass tube was proved for this waveguide types (Fig.1).

For a protection of the waveguide input face and input inner layers during the adjustment stage of the system, a special tube-shaped protector was inserted at the beginning of the delivery system.

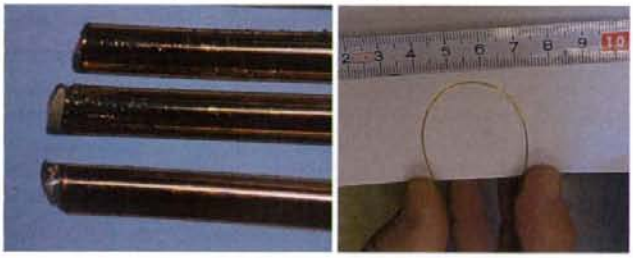

Fig. 1. Photo of COP coated silver hollow glass waveguides with the 250/360 μm diameter.

2.3 Measuring instruments and methods

The characterization was performed for both – the radiation entering into the waveguide, and the delivered one. The laser radiation energy, time dependence, and the spatial structure were measured. For measurement of the energy the two-channel Molectron JD 2000 Joulemeter/Ratiometer with Molectron probes (model No. J25) was used. The waveform was investigated by PIN detector ET-3000 (InGaAs, EOT) connected with the Tektronix 3052B scope. The radiation power was measured by Molectron EPM 2000 power meter with Molectron PM3 probe. The beam spatial structure was monitored by the Electrim CCD camera (EDC-1000HR) or pyroelectric camera (Spiricon Pyrocam III).

Due to the very high stability of the generated laser radiation, the transmission of the waveguide system was calculated from consecutively performed measurement of the input and output energy before and behind the waveguide.

3. RESULTS

3.1 Delivery of 1.06 μm Nd:YAG laser radiation

The Nd:YAG laser radiation coherently pumped by the Alexandrite laser generated the fundamental TEM_{00} mode with $M^2 \cong 1$ (Fig.2). The maximum output energy was 0.7 mJ in the pulse with length of 6 ns, the corresponding power was 116.7 kW.

Fig. 2. Output beam spatial structure of 1.06 μm Nd:YAG laser radiation (2D image, Electrim CCD camera EDC-1000HR).

The coupling was realized by an achromatic doublet with a focal length 75 mm. The beam profile was checked behind the focusing optic, and it wasn't changed. The beam diameter in focus plane was measured 32 μm. The investigated waveguides were placed into the protector fixed in the adjustable holder. The energy delivery characteristics summary is in Table 1. The output beam structures behind the waveguides are shown in Figure 3 for 100 μm, and in Figure 4 for 250 μm inner diameter waveguides.

Table 1 – Delivery characteristics of 1.06 μm Nd:YAG laser radiation.

Number of waveguide (inner diameter)	Input energy	Output energy	Transmission
1A6-11-2 (100 μm)	0.49 mJ	0.47 mJ	95.8 %
C25-3-0 (250 μm)	0.68 mJ	0.46 mJ	67.1 %
C25-3-1 (250 μm)	0.68 mJ	0.55 mJ	80.8 %
C25-3-2 (250 μm)	0.68 mJ	0.52 mJ	76.6 %
C25-3-4 (250 μm)	0.68 mJ	0.51 mJ	74.3 %

Fig. 3. Output beam spatial structure of 1.06 μm Nd:YAG laser radiation behind waveguide with 100 μm inner diameter and 10 cm length (2D image, Electrim CCD camera EDC-1000HR).

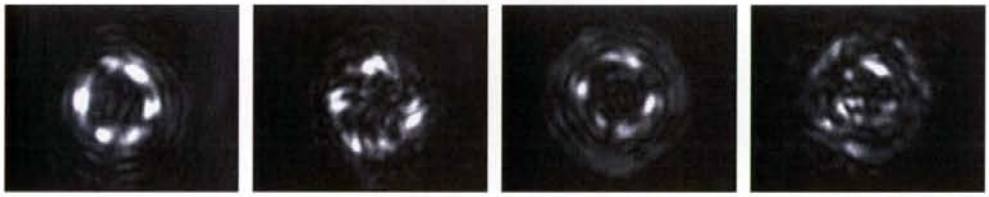

Fig. 4. Output beam spatial structure of 1.06 μm Nd:YAG laser radiation behind waveguides (C25-3-0, C25-3-1, C25-3-2, C25-3-4) with 250 μm inner diameter and 10 cm length (2D image, Electrim CCD camera EDC-1000HR).

3.2 Delivery of 1.34 μm Nd:YAG/V:YAG laser radiation

The output from the diode pumped Nd:YAG/V:YAG laser was fundamental TEM_{00} mode with $M^2 \cong 1$ (Fig. 5). The laser radiation output mean power was 25 mW. The measured pulse length was 6 ns, the corresponding pulse energy and peak power were 0.1 mJ and 16.7 kW, respectively

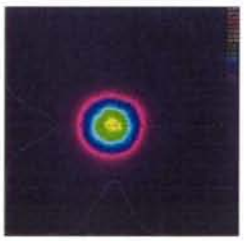

Fig. 5. Output beam spatial structure of 1.34 μm Nd:YAG/V:YAG laser radiation (2D and 3D image - pyroelectric camera Spiricon Pyrocam III).

The delivery measurement was analogous with the previous 1.06 μm Nd:YAG laser case; for coupling the plan-convex lens with focal length 75 mm was used. The energy delivery characteristics are shown in Table 2, as well as the output beam profiles are in Figure 6 and in Figure 7.

Table 2 – Delivery characteristics of 1.34 μm Nd:YAG/V:YAG laser radiation.

Number of waveguide (inner diameter)	Input mean power	Output mean power	Transmission
1A6-11-2 (100 μm)	14 mW	3.5 mW	25.0 %
C25-3-0 (250 μm)	22 mW	12.5 mW	56.8 %
C25-3-1 (250 μm)	22 mW	9.0 mW	40.9 %
C25-3-2 (250 μm)	22 mW	13.0 mW	59.1 %
C25-3-4 (250 μm)	22 mW	13.0 mW	59.1 %

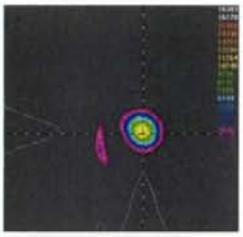

Fig. 6. Output beam spatial structure of 1.34 μm Nd:YAG laser radiation behind waveguide with 100 μm inner diameter and 10 cm length (2D and 3D image - pyroelectric camera Spiricon Pyrocam III).

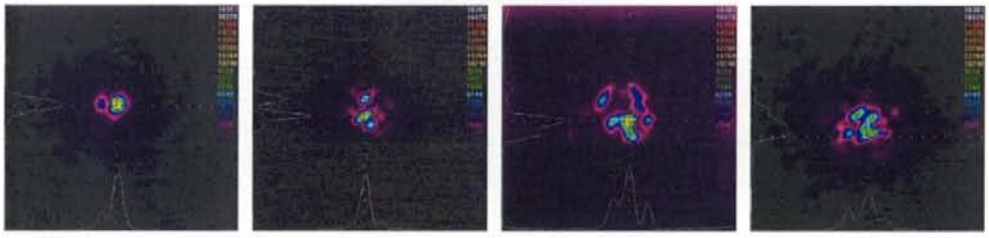

Fig. 7. Output beam spatial structure of 1.34 μm Nd:YAG laser radiation behind waveguide with 250 μm inner diameter and 10 cm length (2D and 3D image - pyroelectric camera Spiricon Pyrocam III).

4. DISCUSSION AND CONCLUSION

In this work, two Nd:YAG laser systems were designed and constructed. The both systems work in Q-switching regime and generated fundamental TEM_{00} mode. The first, Nd:YAG laser passively Q-switched by $LiF:F^{2-}$ saturable absorber was pumped by Alexandrite laser radiation (755 nm, repetition rate 5 Hz) and generated radiation at 1.06 μm wavelength. The maximum output energy (power) and pulse length were 0.7 mJ (116.7 kW) and 6 ns, respectively. The second system was Nd:YAG/V:YAG microchip laser pumped by laser diode and generating the radiation at 1.34 μm wavelength. The output mean power, pulse length, and repetition rate were 25 mW, 6 ns, and 250 Hz, respectively. Corresponding pulse energy and peak power were 0.1 mJ and 16.7 kW, respectively.

As the major goal of this work, the delivery of high power near-infrared radiation (1.06 μm and 1.34 μm wavelength) by 100/190 μm and 250/360 μm thin hollow glass waveguides, and the modification of the beam spatial profile were investigated.

The summary of the energy transmission by the investigated waveguides is in Table 3. The decrease of value transmission on 25 % for wavelength 1.34 μm and 100 μm inner diameter waveguide was probably caused by damage of waveguide inner layers. So the check with another same type of this waveguide is necessary. Nevertheless the complete delivered transmission was more than 55 % and it can be sufficient for some application.

Table 3 - Transmission of radiations by investigated COP/Ag hollow glass waveguides.

Inner diameter	250 μm				100 μm
Number of waveguide	C25-3-0	C25-3-1	C25-3-2	C25-3-4	1A6-11-2
1.06 μm radiation	67.1 %	80.8 %	76.6 %	74.3 %	95.8 %
1.34 μm radiation	56.8 %	40.9 %	59.1 %	59.1 %	25.0 %

The delivered beam spatial structures for waveguides with corresponding inner diameters (100 μm and 250 μm) were similar for both investigated wavelength. From our results it follows that the spatial structure for 100 μm inner diameter waveguide is without significant changes (Fig.2 and Fig.3, Fig.5 and Fig.6).

The 250 μm inner diameter COP/Ag hollow glass waveguides do not keep the input beam fundamental profile. The differences of the input and output structures are shown in Fig.2 and Fig.4, and Fig.5 and Fig.7, for the case of 1.06 μm and 1.34 μm delivered laser radiation, respectively. The fundamental mode was changed into more peaks. The output beam spatial structure was rotated during fine angle adjustment of the waveguide input near the position with the maximum energy delivery.

The following measurement of the output beam structures is going to focus to the longer thin waveguides and to the modification of the delivery properties in the case of waveguide bending. The crucially important parameter will be the radiation losses for bent thin waveguides.

As summarization it can be concluded that the investigated delivery system with 100 μm inner diameter hollow glass waveguide appears as useful for the applications where the defined laser beam structure is required, for example the medical treatment (ophthalmology, microsurgery).

ACKNOWLEDGEMENT

This research has been supported by the Center for Advanced Telecommunications Technology Research Foundations (SCAT) and by grant JSPS No. 17206033, as well as by the Grant of the Czech Ministry of Education No.MSM6840770022 "Laser systems, radiation and modern optical applications".

REFERENCE

1. T. Dostálová, H. Jelínková, M. Miyagi, K. Hamal, and O. Krejsa, "Contact and non-contact laser preparation of hard dental tissues by Er:YAG laser radiation delivered by hollow glass waveguide or articulated arm", in Lasers in Dentistry, Proceedings of SPIE *3593*, 221-217, SPIE, (Washington), 1999.
2. M.Nakazawa, Y. Shi, K. Iwai, Y. Matsuura, X. Zhu, M. Miyagi, "Flexible hollow polycarbonate fiber for endoscopic infrared laser treatment", In: Novel Optical Instrumentation for Biomedical Applications III, Proceedings of SPIE Vol.*6631*, 66311A, 2007.
3. B. Dekel, Z. Barkay and A. Katzir, "The study of waveguides made by diffusion of Br into AgCl substrates and the transmission of mid-IR radiation through these waveguides", Optics Communications, Vol.199 (5-6), 383-388, 2001.
4. David J. Haan; James A. Harrington, "Hollow waveguides for gas sensing and near-IR applications", In: Specialty Fiber Optics for Medical Applications, Proceedings of SPIE Vol.*6596*, 43-49, 1999.
5. M.Němec, H.Jelínková, M.Fibrich, P.Koranda, M.Miyagi, K.Iwai, Yi-Wei Shi, Y.Matsuura, "Modification of mid-infrared radiation spatial structure caused by COP/Ag hollow waveguide", In: Optical Fibers and Sensors for Medical Diagnostics and Treatment Applications VII, Proceedings of SPIE Vol.*6433*, p. 643306, 2007.
6 J. Šulc, H. Jelínková, K. Nejezchleb, and V. Škoda, "Nd:YAG/V:YAG microchip laser operating at 1338 nm", Laser Physics Letters 2(11), pp. 519-524, 2005.

Fabrication of 100-μm-bore hollow fiber for infrared transmission

Katsumasa Iwai[1)], Mitsunobu Miyagi[1)], Yi-Wei Shi[2),*], Xiao-Song Zhu[2)], Yuji Matsuura[3)]

1) Sendai National College of Technology,
4-16-1 Ayashi-chuo, Aoba-ku, Sendai, 989-3128, Japan.
2) School of Information Science and Engineering, Fudan University,
220 Handan road, Shanghai 200433, China
* Email: ywshi@fudan.edu.cn, TEL/ FAX: +86-21-5566-4945
3) Graduate School of Engineering, Tohoku University,
Aramaki Aoba, Aoba-ku, Sendai 980-8579, Japan.

Abstract

Extremely flexible hollow fibers with 100 μm-bore size were developed for infrared laser delivery. The hollow fiber was inner coated with silver and a dielectric layer to enhance the reflection rate at an objective wavelength band. The silver layer was plated by using the conventional silver mirror-plating technique. And a thin dielectric layer was coated for low-loss transmission of Nd:YAG and Er:YAG laser light.

KEYWORD: hollow fiber, small-bore, infrared laser.

1. Introduction

Er:YAG laser, radiating at the wavelength of 2.94 μm, is an effective laser in biomedical field for incision and ablation. Low-loss hollow optical fiber for delivering Er:YAG laser light has been successfully developed [1-3], and the application of the Er:YAG laser is rapidly expanding in almost all the subfields in medicine. In many medical applications, there is a critical requirement for ultra-thin infrared fiber. Hollow fiber with an outer diameter less than 200 μm is a typical one. In dentistry, an edged tool with 160 μm outer diameter, being called *the Fiber*, is often used to treat the root of a bad tooth so as to keep the bad tooth from being removed. The infection parts at the root can be removed by using *the Fiber*. However, *The Fiber* is easily becoming blunt and the treatment time has to be prolonged. It is possible to shorten the treatment time to irradiate the infected part by using Er:YAG laser light. Therefore, the development of a patient-friendly thin hollow fiber for delivering

Optical Fibers and Sensors for Medical Diagnostics and Treatment Applications VIII,
edited by Israel Gannot, Proc. of SPIE Vol. 6852, 68520S, (2008) · 1605-7422/08/$18
doi: 10.1117/12.767934

ErYAG laser light has been one of the important research themes in laser dentistry.

We have been working on the research and development of infrared hollow fibers with bore-size ranging from 250 μm to 1000 μm for medical applications. Correspondingly, the outer diameters are ranging from 320 μm to 1500 μm. The hollow fiber was inner coated with a dielectric and a silver layer to reduce the transmission loss and obtain high-performance properties such as multi-wavelength delivery [4-6]. In the minimally invasive treatment of the tooth root by using an endoscope, we are trying to introduce a thinner hollow fiber for delivery the Er:YAG laser light. In this paper, we report on the fabrication of extremely flexible, low-loss, infrared hollow fiber with 100 μm-bore size.

2. Fabrication of the silver-coated ultra-thin hollow fiber

In the fabrication of a small-bore hollow fiber, a silica capillary tube is used as the base tube. The inner/outer diameters of the silica capillary are 100/170 μm, including a polyimide protective coating with 12 μm thickness on the outside surface to keep its flexibility and durability. The capillary can be safely bent with a bending radius as small as 2.5 mm, which is much more flexible than the fiber with 250 μm inner diameter that we developed before [4]. We coat silver layer and a dielectric layer as the high-reflection films on the inner surface of the capillary. In order to obtain a low-loss property at an objective wavelength, we have optimized the film thickness of the dielectric layer [7]. For the dielectric material, we used organic material such as cyclic olefin polymer (COP) and inorganic material such as SiO_2 (OC300 for the trade name of the coating material) [8].

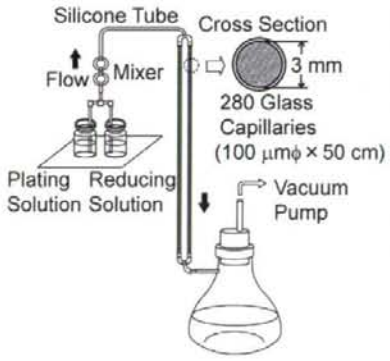

Figure 1. Experimental setup for depositing a silver layer inside the silica capillary.

Figure 1 shows the experimental setup for silver plating in the capillary tube. The silica capillary was with a length of 50 cm and an inner diameter of 100 μm. In the plating process, a silver film with the thickness of around 0.1 μm was formed. As shown in fig. 1, the plating solution and the reducing solution were forced to flow through the silica capillary. The two solutions were thoroughly mixed in the mixer. Silver reduced in the chemical reaction adhered on the inner surface and thus formed a silver layer. However, in fabrication of small-bore hollow fibers the flowing rate of the solutions became so lower that the two solutions could not be fully mixed before entering the capillary. This caused rough silver surface and even get stuffed by silver in the thin capillary.

In this research we have improved the fabrication techniques to solve these problems.

a. An $SnCl_2$ water solution was used as an activation solution to initialize the inner surface of the capillary before the silver-mirror plating. With the pretreatment, the reducing process was much more rapid and the silver layer could be formed in a much shorter time.
b. In order to increase the flowing rate, we made two bundles with 280 pieces of silica capillary (inner/outer diameters of 100/170 μm and length of 50 cm) to increase the cross-sectional area. The bundles were connected to silicone tubes with inner/outer diameters of 3/5 mm.

Concerning the silver plating parameters used up to now in the fabrication of hollow fibers with 700 μm bore-size, we targeted the flowing rate of the solutions at 15 ml/min. To achieve the target, we paralleled two bundles each with 280 pieces of capillary. The flowing rate was measured 14.5 ml/min. The silver mirror reaction process lasted for 3 minutes. An afterwards-treatment to evaporate water in the hollow core was also conducted, the fiber were kept in a 150°C furnace for 30 minutes, while nitrogen gas flowing through the hollow core at the rate of 300 ml/min.

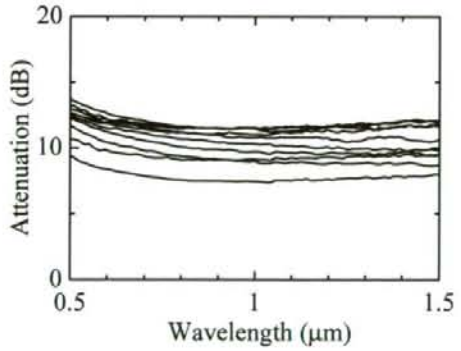

Figure 2. Loss spectra in the VI-NIR regions for the silver-coated hollow fiber with 100 μm-bore size and 35 cm length. The fiber was excited with a Gaussian beam with FWHM 10.6 °

Figure 2 shows the loss spectra in the visible and the near infrared (VI-NIR) regions for the hollow fibers with an inner silver layer. In the measurement, the fiber was excited by a Gaussian beam with a full width at half maximum (FWHM) of 10.6°. It can be seen that the attenuation of the fibers distributed in a relatively large range. The loss difference between the minimum and the maximum was 4.3 dB. The large difference might be caused by the imperfection in the fiber bundle preparation. When we made the bundle with 280 pieces of hollow fibers, it was difficult to keep the end face tidiness. Therefore, the flowing rate of the solutions in each fiber could be largely different. However, the lowest attenuation for the fiber with 35 cm length was 7.5 dB at the wavelength of 1 μm for Nd:YAG laser light, which was a quite low attenuation for the thin hollow fiber. Furthermore, the fabrication method can produce 560 pieces of silver-coated hollow fibers in one silver mirror reaction process, which is important to a batch production.

Up to now, we have fabricated hollow fibers with various inner diameters ranging from 250 to 1000 μm based on the commercially available silica capillary (inner diameters of 250, 320 540, 700 and 1000 μm). We used the cutback method to measure the attenuation properties of the hollow fiber. A reference fiber with 10 cm length and a measured fiber with 30 cm length were used. The outputs of the 10 cm long fiber and the 30 cm long fiber were measured and recorded. Then the loss spectrum of a 20 cm long fiber was calculated. The loss spectra in VI-NIR regions for the hollow fiber with various inner diameters were measured and calculated. Figure 3 shows their losses at the wavelength of 1 μm (excited by a Gaussian beam with FWHM=10.6°).

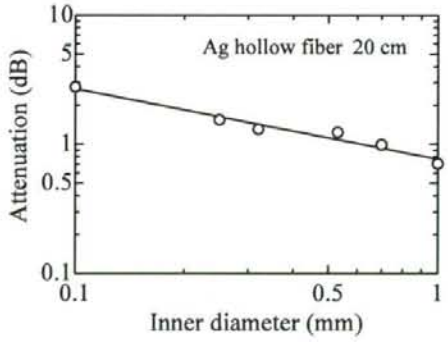

Figure 3. Transmission attenuation of the hollow fiber with various inner diameters. The fiber is with the length of 20 cm. The attenuation was measured at the wavelength of 1 μm and the fiber was excited by a Gaussian beam at FWHM 10.6°.

Theoretically, the loss of the hollow fiber is in inverse proportion to the cube of the inner diameter. The theory has been well proved by the loss properties of the hollow fiber produced before. We can see from fig. 3 that the loss of the 100 μm-bore hollow fiber is on the loss-property line of hollow fiber with larger bore-size. We can conclude that the small-bore hollow fiber attained the same low-loss level as these fibers we had produced before.

3. The dielectric film coating for the thin hollow fiber

We coated dielectric film on the silver layer to reduce transmission loss. For the dielectric material, we used cyclic olefin polymer (COP) and OC300 (SiO_2) [8]. For COP film coating, a COP cyclohexane solution with a concentration of 8.5 wt% was used. The silver-coated hollow fiber was kept straight and vertically fixed on a stable stage. The COP solution was flown through the silver-coated hollow fiber with a constant speed. The flow speed of the COP solution was set at around 10 cm/min. As the afterwards treatment to evaporate the solvent cyclohexane in the liquid-phase film, we flew nitrogen gas through the hollow core at the flowing rate of 100 ml/min. Then a COP film was formed on the silver layer. However, the COP solution tended to be stuffed easily due to the ultra thin hollow core.

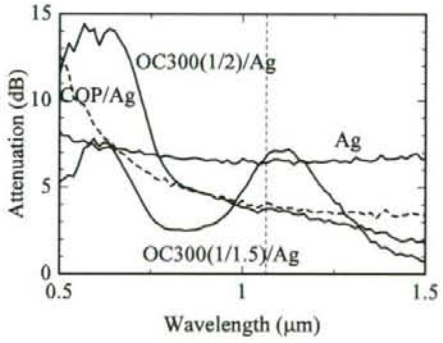

Figure 4. Loss spectra of COP/Ag and OC300/Ag hollow fibers (100 μmϕ×10 cm) in VI-NIR regions (FWHM = 10.6°). OC300 (1/2) and OC300 (1/1.5) mean that 10:1:20 and 10:1:15 mixing rate solutions were used in the fabrication.

We also tried to use an inorganic material OC300 [8] as the dielectric film. OC300 is the trade name of the coating material. It is a semi-inorganic polymer based on the structural unit R_2SiO, where R is an organic group. The material is characterized by wide-range thermal stability, water repellence, and physiological inertness. The OC300 coating material was originally developed for protecting the

surface of a building or floor. It is a commercially available product and sold in a two-solution set. One is the main paint solution, and the other is a hardener. The two solutions are mixed at a certain rate. When the mixed solution is painted on a smooth surface, a solid SiO_2 film can be formed at the room temperature with the catalysis of water in the air.

There is another solvent that can be used to dilute the mixed solution. It is possible to modify the viscosity of the mixed solution by a certain amount of the solvent. In this research, the mixing rate among these three solutions (the main paint solution, the hardener and the solvent) was 10:1:20 or 10:1:15. The coating method was the same as what we used for COP coating. The flowing speed of the solution was 10 cm/min. After the liquid-phase coating, the fiber was treat at the room temperature with nitrogen gas flowing through the hollow core for 1 hour. The OC300-coated silver (OC300/Ag) hollow fiber was fabricated. Comparing with the COP solution, the OC300 solution has a lower viscosity. The OC300 solution moves smoothly inside the thin hollow core without stuffing at halfway. Therefore, it is comparatively easier for the OC300 coating in the small bore hollow fiber. Figure 4 shows the loss spectra of the hollow fibers in the VI-NIR regions. The fibers are 10 cm long, with 100 μm bore-size and excited with a Gaussian beam with FWHM at 10.6°.

Comparing with the silver-coated hollow fiber, the COP/Ag and OC300 (1/2)/Ag hollow fibers attained low loss at the wavelength of 1 μm (OC300 (1/2)/Ag means a fiber used the 10:1:20 rate solution in its fabrication). The COP/Ag hollow fiber (dashed curve) had a COP film with a thickness of 0.1 μm. It is possible to deliver Nd:YAG laser light with low-loss. OC300 (1/2)/Ag hollow fiber had OC300 film with a thickness of 0.15 μm. It is also obtained low-loss at the wavelength of Nd:YAG laser light. To deliver the Er:YAG laser light radiating at the wavelength of 2.94 μm, a thicker dielectric film is required. Normally a solution with higher concentration is need for a thicker film coating. Because COP solution has a high viscosity, it is almost impossible to drive a thicker solution through the 100 μm bore hollow core. While OC300 solution has a low viscosity, we increase the concentration by the mixing rate of 10:1:15. As seen in fig. 4, the OC300 film is evaluated as 0.25 μm. and the fiber was expected to have a low-loss property at the wavelength of 2.94 μm for the Er:YAG laser light. Furthermore, the clear interference peaks in the VI-NIR regions indicated that a uniform and smooth OC300 film had been achieved.

In order to evaluate the transmission loss for the Er:YAG laser light of the 100 μm bore hollow fiber, we used a tapered coupler to couple the laser light into the small core. In the measuring experiments, the fiber was 10 cm long with a 100 μm bore-size. The tapered coupler was 1 cm long and the inner diameters of the input and output ends were 700 and 100 μm, respectively. The Er:YAG laser was set at an output mode with 10 Hz repetition rate, 300 μs pulse width and 33 mJ energy per pulse. The tapered coupler was obtained by the glass-drawing method from a silica capillary with 700 μm bore-size [9]. The coupler was 6 cm long, in which 5 cm length was a uniform 700 μm bore

hollow fiber and the rest 1cm tapered off to 100 μm bore-size gradually. The Er:YAG laser light was coupled into the 100 μm bore hollow fiber with the tapered coupler. The measured losses for the thin hollow fibers are summarized in table 1. The tapered coupler itself has a loss of 1.4 dB. And the minimum loss for the 100 μm bore hollow fiber was OC300 (1/1.5)/Ag hollow fiber, which was still as high as 8.8 dB. This might be cause by the tapered coupler. Because the taper coupler excited more high-ordered modes in the measured thin hollow fiber, which are of much higher attenuation coefficients than those of the low-ordered modes. It is necessary to optimize the shape of the tapered coupler to reduce the loss of the thin hollow fiber.

Table 1 Transmission characteristics for Er:YAG laser

	Energy (mJ)		Loss (dB)
	Input	Output	
Ag	24	0.7	15.3
COP/Ag	24	1.4	12.3
OC300 (1/2)/Ag	24	1.8	11.2
OC300 (1/1.5)/Ag	24	3.2	8.8

4. Conclusion

Small-bore hollow fiber with 100 μm inner diameter was fabricated. Comparing with the loss properties of the hollow fibers with larger bore-size produced before, the thin hollow fiber obtained low-loss property. The COP and OC300 were used as the dielectric film. For a Nd:YAG hollow fiber, dielectric film thickness of around 0.1 μm was coated and the loss was much lower than a silver-coated hollow fiber. A thicker OC300 film with 0.25 μm was also successfully coated, the fiber attained low-loss for Er:YAG laser light radiating at the wavelength of 2.94 μm. The loss for the 100 μm bore, 10 cm length OC300/Ag hollow fiber was 8.8 dB. The OC300 coated thin hollow fiber are of low-loss property, extreme flexibility and high durability, which is promising in many applications.

Acknowledgements

This research is supported by the Ministry of Education, Science, Sports and Culture of Japan through a Grant-in-Aid for Scientific Research (A) (17206033) and (B) (19760240) 2007, as well as by the National Nature Science Foundation of China (60608013) and the Shanghai Pujiang program (07pj14012).

Reference

1. J. Raif J, M. Vardi, O. Nahlieli, and I. Gannot, "An Er:YAG laser endoscopic fiber delivery system for lithotripsy of salivary stones," Laser in Surgery and Medicine **38**, 580-587 (2006).
2. S. Sato, Y. W. Shi, Y. Matsuura, M. Miyagi, and H. Ashida, "Hollow waveguide based nanosecond, near-infrared pulsed laser ablation of tissue," Lasers in Surgery and Medicine **37**, 149-154 (2005).
3. V. S. Johnson, B. Bowden, and J. A. Harrington, "Polymer/metal sulfide coated hollow waveguides for delivery of Er:YAG laser radiation," Proc. of SPIE **6433**, 64330E-1-64330E-8 (2007).
4. Y. Abe, Y. W. Shi, Y. Matsuura, and M. Miyagi, "Flexible small-bore hollow fibers with an inner polymer coating," Opt. Lett. **25**, 150-152 (2000).
5. M. Nakazawa, Y. W. Shi, Y. Matsuura, K. Iwai, and M. Miyagi, "Hollow polycarbonate fiber for Er:YAG laser light delivery," Opt. Lett. **31**, 1-3 (2006).
6. K. Iwai, Y. W. Shi, M. Miyagi, and Y. Matsuura, "Improved coating method for uniform polymer layer in infrared hollow fiber," Opt. & Laser Technol. **39**, 1528-1531 (2007).
7. M. Miyagi and S. Kawakami, "Design theory of dielectric-coated circular metallic waveguides for infrared transmission," IEEE J. Lightwave Technol. **LT-2**, 116-126 (1984).
8. K. Iwai, Y. W. Shi, M. Miyagi, X. S. Zhu, and Y. Matsuura, "Hollow infrared fiber with an inorganic inner coating layer with high durability," Proc. of SPIE **6433**, 64330L-1-64330L-7 (2007).
9. S. Narita, Y. Matsuura, and M. Miyagi, "Tapered hollow waveguide for focusing infrared laser beams," Opt. Lett. **32**, 930-932 (2007).

2E08

赤外レーザ光同時照射による軟組織の蒸散・凝固効果

○岩井克全*，渡邊智紀**，松浦祐司***
*仙台電波工業高等専門学校，**東北大学大学院工学研究科，***東北大学大学院医工学研究科

1. はじめに

複合赤外レーザ光を用いた高効率レーザ治療が期待されている。我々のグループでは、高エネルギー赤外レーザ光を同時伝送可能な中空ファイバを用い、Er:YAG レーザ光(波長 2.94 μm)と Ho:YAG レーザ光(波長 2.1 μm)の同時照射による硬組織の結石破砕応用を試みてきた[1]。本研究では、複合レーザ光を用いた更なる医療応用として軟組織の切開手術に着目し、2 波長赤外レーザ光を軟組織へ照射した際の蒸散・凝固効果について検討した。

2. 2 波長同時伝送システム

図 1 に Er:YAG レーザ光 (パルス幅 350 μs)と Ho:YAG レーザ光 (パルス幅 250 μs)の同時伝送システムを示す。各光源から照射された光は、ZnSe 多層膜ビームスプリッターを透過および反射し、焦点距離 76 mm の CaF_2 レンズで集光され、テーパ入射結合器 (入射端内径 1.1 mm、出射端内径 0.7 mm、長さ 80 mm)に入射される。テーパと中空ファイバ(内径 700 μm)の内面には、銀層と環状オレフィンポリマー (COP)を内装している。COP 膜厚は、2 波長同時伝送に最適な 0.28 μm とした。ファイバ先端には平凸型シーリングキャップを装着している。

3. 2 波長同時照射による軟組織の蒸散・凝固特性

Er:YAG レーザ光と Ho:YAG レーザ光を、空気中で軟組織(牛肉)へ照射する。キャップ先端と軟組織表面を接触させた状態で固定し、照射時間 5 秒とし、各光源の繰り返し周波数およびキャップ先端からの出射エネルギーを変化させた。軟組織へ 2 波長同時照射した結果を図 2 に示す。Er:YAG レーザ光は蒸散深度が深く、Ho:YAG レーザ光は凝固層が厚いことが分った。また 2 波長同時照射により、蒸散部と凝固層が形成されており、切除と同時に止血が可能と思われる。

次に、水中における蒸散・凝固特性を測定する。蒸散部周辺に明確な凝固層が形成されるように Er:YAG レーザ光(5Hz、100mJ)、Ho:YAG レーザ光(10Hz、100mJ)を軟組織へ同時照射する。図 3 に照射時間に対する蒸散・凝固深度を示す。水中においても蒸散部および凝固層は形成された。空気中で照射時間を長くすると蒸散・凝固深度は深くなるが、水中では数十秒照射し続けても、蒸散・凝固深度はほとんど変化しないことが分った。

4. まとめ

Er:YAG レーザ光と Ho:YAG レーザ光の中空ファイバ同時伝送システムを用いて、軟組織の蒸散・凝固効果を測定した。2 波長同時照射により、切除と止血が同時にでき、水中においても蒸散部および凝固層を形成できることが分った。

参考文献

1) 岩井,宮城, 松浦 : 平成 19 年度電気関係学会東北支部連合大会, 1H11 (2007).

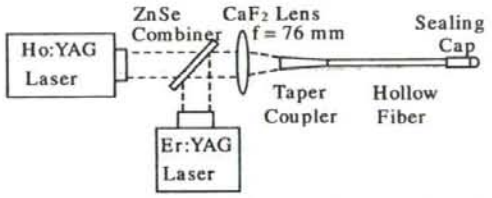

図 1　中空ファイバを用いた Er:YAG と Ho:YAG レーザ光の同時伝送システム

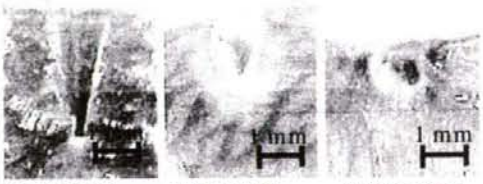

(a) Er:YAG (10Hz、100mJ)　(b) Er:YAG (5Hz、50mJ) + Ho:YAG (10Hz、100mJ)　(c) Ho:YAG (10 Hz、100mJ)

図2　軟組織への Er:YAG と Ho:YAG レーザ光照射
但し、軟組織は牛肉、照射時間 5 秒。

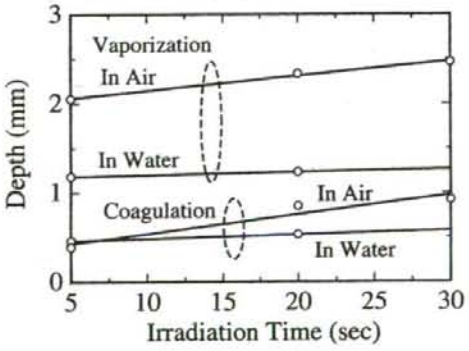

図3　2 波長同時照射による軟組織の蒸散・凝固効果
但し、軟組織は牛肉、Er:YAG (5 Hz, 100 mJ) と Ho:YAG (10Hz, 100mJ)を同時照射。

赤外レーザ用内径 100 μm 中空ファイバの製作

Fabrication of 100-μm-bore Hollow Fiber for Infrared laser

岩井 克全[*1] 宮城 光信[*1] 石 芸尉[*2] 松浦 祐司[*3]
Katsumasa Iwai Mitsunobu Miyagi Yi-Wei Shi Yuji Matsuura

[*1] 仙台電波工業高等専門学校 [*2] 復旦大学 情報科学工学部 [*3] 東北大学大学院 医工学研究科
Sendai National College of Tech. School of Info. Science and Eng., Fudan Univ. Graduate School of Biomedical Eng., Tohoku Univ.

1. はじめに

筆者らは、効率よい歯科根管治療のために、内径 100 μm 超細径中空ファイバの導入を提案し、以前の研究では、低損失な超細径銀中空ファイバの製作に成功した[1)]。今回は、送液法を用い、より低損失な光学ポリマー内装超細径銀中空ファイバの製作を行ったので報告する。

2. 製作と特性評価

ポリマー膜の形成は送液法により行う。図 1 に光学ポリマー内装超細径銀中空ファイバの製作装置を示す。中空ファイバの内径が細くなると、ポリマー溶液の流速が急激に速くなる。そのため、送液系の接続点におけるチューブ径の違いにより、送液速度が変化し、ファイバ上・下部で膜厚変動を生じると思われる。そこで、通常用いる内径 700 μm の接続チューブを内径 530 μm と 230 μm の 2 段階接続(図 1 左参照)に改良することにより、接続点における送液速度の変動を抑え、均一なポリマー膜形成を行う。

光学ポリマーに、環状オレフィンポリマー (COP)と室温湿気硬化型特殊無機塗料 OC No.300 クリアー (OC300)を用いる。Er:YAG レーザ光 (波長 2.94 μm)用の細径中空ファイバを製作する場合、濃いポリマー溶液が用いられる。その際、濃い溶液では粘度が上昇し、送液速度が大きく変化する。そこで、安定した送液を行うために、送液系をダミーチューブで循環させ、ポリマー溶液を上・下部から力を加える手法を用いる。内径 100 μm、長さ 30 cm の銀中空ファイバに光学ポリマーを送液速度 10 cm/min で送液し、その後、窒素ガスを流量 100 ml/min で流しながら、室温乾燥を 1 時間行った。

図 2 に製作した内径 100 μm 光学ポリマー内装銀中空ファイバ (長さ 10 cm)の可視-近赤外波長帯における損失波長スペクトル (FWHM10.6 ° のガウスビームで励振)を示す。比較として、内径 100 μm 銀中空ファイバ (長さ 10 cm)も示す。溶液濃度 8.5wt%の COP 溶液を用いて、Nd:YAG レーザ光 (波長 1.064 μm)用中空ファイバの製作に成功したが、これ以上の厚膜化は、COP 溶液の粘度が高く困難であった。OC300 溶液は COP 溶液と比較して粘度が低く、溶液濃度 38 wt%を用いて、Er:YAG レーザ光伝送に適した膜厚を成膜することに成功した。明確な干渉ピークが見られ、ファイバ内に均一な光学膜を形成できていると思われる。

3. まとめ

超細径中空ファイバの光学ポリマーの成膜法について検討を行い、Nd:YAG レーザ光および Er:YAG レーザ光用の低損失な内径 100 μm、長さ 10 cm の光学ポリマー内装銀中空ファイバの製作に成功した。

参考文献
1) 岩井、宮城、石、松浦、信学ソ大、C-3-32 (2007).

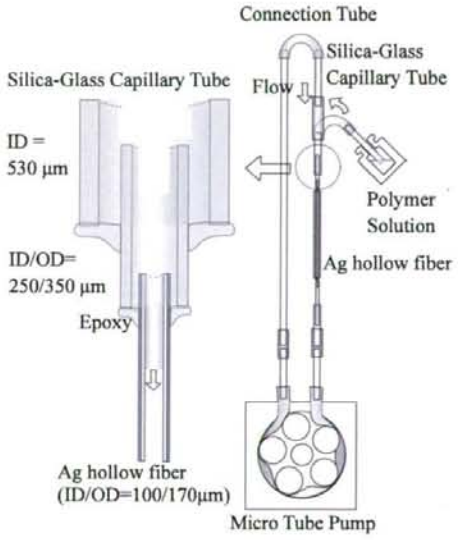

図 1 内径 100 μm 光学ポリマー内装銀中空ファイバ製作装置

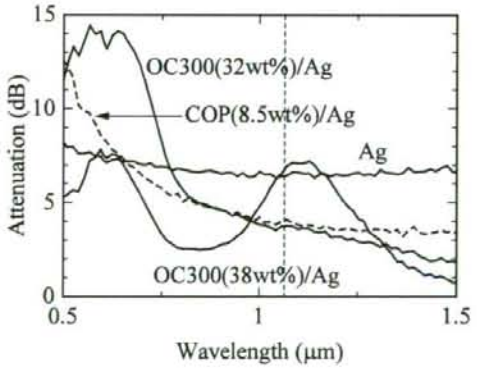

図 2 内径 100 μm 中空ファイバの可視-近赤外の損失波長スペクトル(FWHM10.6 °のガウスビームで励振)

Er:YAG, Ho:YAG レーザの同時照射による硬組織の高効率蒸散

Radiation of Er:YAG and Ho:YAG lasers for highly efficient ablation of hard tissues

渡邊 智紀　　*岩井 克全　　松浦 祐司
Tomonori Watanabe　Katsumasa Iwai　Yuji Matsuura
東北大学大学院工学研究科　　*仙台電波工業高等専門学校
Graduate school of Engineering, Tohoku University　Sendai National College of Technology

1. はじめに

歯牙・結石などの生体硬組織の切削・蒸散治療には Ho:YAG（Cr,Tm,Ho:YAG）レーザや Er:YAG レーザが有用とされている．これらのレーザは組織に含有される水分にレーザ光が吸収されることにより蒸散を行うが，充分な切削効果を得るには大きなパルスエネルギー及び平均パワーを必要とする．蒸散時の熱の発生を抑えるためにより低エネルギーで蒸散を行う手法として，我々のグループは上記の二波長レーザを同時照射することで，相互作用による高い切削効果が得られることを見出した．そこで本研究では，同時照射する二波長パルスの照射タイミングを制御することで，生体硬組織の切削・蒸散効率を向上させるための最適な条件について検討する．

2. 二波長パルスレーザの同時照射系

硬組織のサンプル照射実験に用いた実験系を図 1 に示す．Ho:YAG（λ=2.1 μm）と Er:YAG（λ=2.94 μm）をビームスプリッタを用いて同軸とし，中空光ファイバに入射後，レンズキャップにより集光させサンプルに照射・切削を行った．各レーザのパルスは外部トリガーにより制御され，トリガーパルスに遅延を与えることで，二波長パルスの照射パルス遅延をμsec オーダーで制御している．照射サンプルは直径 4~6 mm のアルミナ（Al_2O_3）セラミックボールとした．

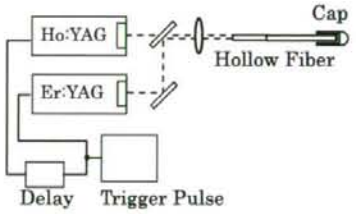

図 1　二波長レーザ同時照射系

3. タイミング制御による切削結果

研磨したアルミナボールの面に対し垂直にレーザを照射・切削し，その切削幅および深さを計測した．各レーザの繰り返し周波数を 3 Hz，パルスエネルギーを 100 mJ とした。二波長レーザを同時照射した場合，切削幅は照射パルス遅延に関わらずほぼ一定の値となったが，切削深さは照射パルス遅延により大きく変動することがわかった．図 2 は，二波長パルスの照射タイミング（Er:YAG に対する Ho:YAG の遅延時間）に対する切削深さ特性を示す．Ho:YAG に対し Er:YAG レーザを 200~300 μsec 遅延させたときに最も大きな切削効果が得られ，パルスエネルギー200mJ とした場合の Er:YAG レーザ照射と比較しても充分鋭い切削が観測された．また二波長パルス間隔をパルス幅（~150 μsec）に対して充分に広い 50000 μsec に設定した場合と比較しても高い切削効果が得られていることから，同時照射による効果は明らかである．

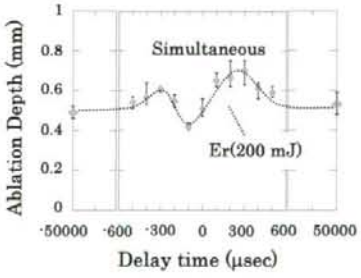

図 2　照射タイミングによる切削深さ特性

本現象を検討するため，切削時のアルミナボール表面の様子を高速度カメラにより観測した．図 3 はそれぞれ(a)Er:YAG のみ，(b)Ho:YAG のみ，(c)同時照射で Er:YAG を 200 μsec 遅延・照射後に撮影した画像である．Er:YAG のみで切削を行った場合，アルミナ表面より微粉末が煙霧状に噴出してくるが，Ho:YAG を先行させた場合は比較的大きな切削片の噴出が観測された．先行した Ho:YAG により水分を含有する組織が瞬間的に加熱された結果，水に対する Er:YAG の吸収率が低下し，浸透深さが増加したためではないかと考えられる．一方で Ho:YAG に対し，Er:YAG を同時または 100 μsec 程度遅延した場合には同様な効果は観測されなかった．これは Er:YAG 照射で発生した煙霧状の切削片により，遅延した Ho:YAG のエネルギーの大半が散乱したためと考えられる．

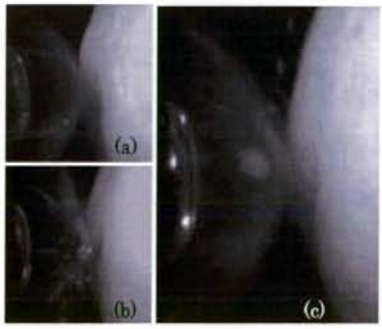

図 3　サンプル表面の切削の様子(a)Er, (b)Ho, (c)Ho+Er(200 μsec 遅延)

I312aIII06

CO_2 レーザー光伝送用無機薄膜内装中空ファイバの製作

Fabrication of Hollow optical fiber with an inorganic inner coating layer for CO_2 laser light delivery

○岩井克全, 宮城光信, 石芸尉[A], 朱暁松[A], 松浦祐司[B] (仙台電波工業高等専門学校, [A]復旦大学, [B]東北大学)
Katsumasa Iwai, Mitsunobu Miyagi, Yi-Wei Shi[A], Xiao-Song Zhu[A], Yuji Matsuura[B]
(Sendai National College of Technology, [A]Fudan University, [B]Tohoku University)

1. はじめに

手術用器具による感染症の危険性を減ずるために, 滅菌処理のオートクレーブに耐えうるファイバが必要である. これまでに無機薄膜 (IM)を内装することで耐久性に優れた Er:YAG レーザー (波長 2.94 μm)用中空ファイバ[1]の製作に成功した. 本研究では, 形成外科等で応用が展開されている CO_2 レーザー (波長 10.6 μm)用無機薄膜内装銀 (IM/Ag)中空ファイバの製作を行い, その伝送特性ならびにオートクレーブに対する耐久試験について述べる.

2. CO_2 レーザー用無機薄膜内装銀中空ファイバの製作

シロキサン (Si-O 結合)硬化薄膜を形成するために, 2 液湿気硬化型無機溶液を用い, 銀中空ファイバ (内径 1 mm, 長さ 10 cm)に, 送液速度 1.6 cm/min で送液を行い, 窒素雰囲気で室温乾燥を行った. 図 1 に無機溶液の濃度に対する無機薄膜の膜厚を示す. CO_2 レーザー用の最適膜厚は 1.59 μm であり, 濃度 68wt%を用いるとよいことが分るが, 実際は膜の吸収損失があるため, 濃度 65wt%を用いた膜厚 1.23 μm 程度の無機薄膜内装銀中空ファイバが低損失であった.

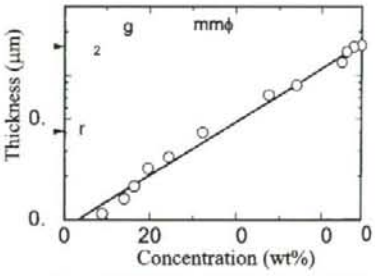

図 1 無機溶液の濃度に対する膜厚

3. CO_2 レーザー光伝送特性とオートクレーブ耐久試験

製作したファイバのオートクレーブ耐久試験を行った. オートクレーブの条件は, 滅菌温度 135℃, 滅菌時間 3min, 最高圧力 0.26 MPa を用いた. オートクレーブのサイクル回数に対する CO_2 レーザー光 (入射パワー100 mW, 連続波)の伝送特性を図 2 に示す. 4 回で銀中空ファイバの損失は増加したが, 無機薄膜 (膜厚 1.23 μm)内装中空ファイバは, 6 回処理しても 80%程度伝送可能であり, その耐久性が確認された.

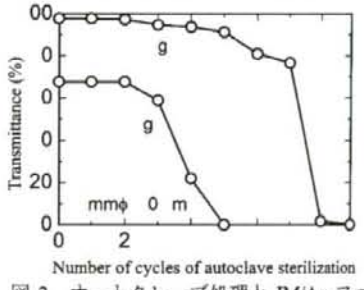

図 2 オートクレーブ処理と IM/Ag ファイバの CO_2 レーザー光伝送特性

4. まとめ

内径 1 mm, 長さ 10 cm の CO_2 レーザー用無機薄膜内装銀中空ファイバの製作を行い, オートクレーブ耐久試験を行った. オートクレーブを 6 回程度 行っても CO_2 レーザー光を低損失に伝送できる中空ファイバの製作に成功した.

参考文献 1) 岩井, 石, 宮城, 朱, 松浦, 第 28 回レーザー学会学術講演会, I6-31pV17 (2008).